

## DIVERSITY OF THE LASER DIRECT MACHINING OF MATERIALS: EXPERIMENTS AND RESULTS

Elena MOCANU<sup>1</sup>, Paul E. STERIAN<sup>2</sup>

**Rezumat.** Scopul articolului de față este să prezinte câteva aspecte noi privind prelucrarea cu laserele a unor materiale. Aplicațiile micromașinilor sunt extrem de diverse și, de aceea, folosesc o paletă largă de lasere în scopul obținerii, în fiecare caz, a unor rezultate optime și a unei economii semnificative. Pentru dezvoltarea acestor noi aplicații este critic să avem, acces la un portofoliu cuprinzător de produse laser, ca și la aplicațiile de dezvoltare suport, pentru a determina cea mai bună soluție pentru o anumită sarcină. Încercăm să prezentăm câteva aplicații industriale ilustrate cu rezultate ale experimentelor efectuate de autori.

**Abstract.** The goal of this study is to present some important updates regarding the laser machining of different materials. Micromachining applications are extremely diverse and therefore utilize a wide range of lasers in order to achieve optimum results and economy in each case. For those developing new applications, it is therefore critical to have access to a comprehensive portfolio of laser products, as well as applications development support, in order to determine the best solution for a particular task. We are trying to expose some industrial applications and the solutions for them, illustrated with results of the authors experiments.

**Keywords:** Laser micromachining, thermal diffusion, fiber laser, laser patterning, solar cells, nonlinear absorption

### 1. Introduction

A complete understanding of laser interaction with materials is still a matter of trials and adjustments. "A solution looking for a problem" is how many scientists described the first working laser, set up by Theodore Maiman in 1960. The gain medium used by Maiman was ruby ( $\text{Cr}^{3+}:\text{Al}_2\text{O}_3$ ), which is sapphire ( $\text{Al}_2\text{O}_3$ ) with a small number of aluminium ions ( $\text{Al}^{3+}$ ) replaced by chromium ions ( $\text{Cr}^{3+}$ ). De Maria *et al* produced the first ultrashort pulses just six years after Maiman's first laser was demonstrated. In addition to ultrashort pulse duration, ultrashort pulses have a broad spectrum, high peak intensity and can form pulse trains at a high repetition rate. The real physical processes of laser beam interaction (drilling, cutting, or welding) with materials are very complex. Problem of laser interaction with materials presents many difficulties, both from modeling as well as from experimental sides.

<sup>1</sup> Academic Center for Optical Engineering and Photonics, University "Politehnica" of Bucharest, 77206, Romania.

<sup>2</sup> Prof. Dr. Eng., Faculty of Applied Sciences, University "Politehnica" of Bucharest, Romania; full member of the Academy of Romanian Scientists (sterian@physics.pub.ro).

One would expect a reasonable description of the main phenomena occurring during laser interaction, but this is complicated because many of physical processes equally contribute to the development of conservation equations, producing draw back because of a great complexity of the equations to be solved. In most instances, this leads to formulation of a model needed to be solved numerically. A lack of pertinent experimental data to compare with, forces one to simplify some equations and use previous analytical and computational work done in this filed.

- (1) Define the laser energy;
- (2) Characterize the laser energy coupling with the target material;
- (3) Find necessary properties of the materials;
- (4) Analyze and simplify the physical phenomena to develop the governing equations;
- (5) Setup boundary conditions, write the governing equations, and develop a computer program.

## 2. Mathematical Models

Micromachining applications are extremely diverse and therefore utilize a wide range of lasers in order to achieve optimum results and economy in each case. For those developing new applications, it is therefore critical to have access to a comprehensive portfolio of laser products, as well as applications development support, in order to determine the best solution for a particular task.

The first step in laser material processing is the coupling of laser radiation to the material's electrons. This happens by the absorption of photons from the incident laser beam to the material's electrons that are promoted to states of higher energy. The major effect is to convert electronic energy into heat. This heat is the one that is useful in all surface treatment applications.

Usually, the deposited energy of a laser irradiation is converted into heat on a time scale shorter than the pulse duration of laser interaction time, because the free carrier absorption (by conduction band electrons) is the primary route of energy absorption in metals and this is transferred to the lattice by electron-phonon interaction. The resulting temperature profile depends on the deposited energy profile and thermal diffusion rate.

The laser energy coupling depends upon a few parameters:

- $n$ , the complex refractive index  $n = n(1+i \cdot k)$  (1)

- $k$ , the attenuation index

- $R$ , reflectivity:  $R = \frac{n^2(1+k^2)+1-2n}{n^2(1+k^2)+1+2n}$  (2)

- $\alpha$ , absorption coefficient  $\alpha = \frac{4\pi k}{\lambda}$  (3)
- $d$ , penetration depth  $d = \frac{1}{\alpha}$

Thermal diffusivity (D) is related to thermal conductivity (k) and specific heat ( $C_p$ ) as it follows:

$$D = \frac{k}{\rho C_p}, \text{ where } \rho \text{ is the density.} \quad (4)$$

The vertical distance (z) over which heat diffuses during the pulse duration ( $t_p$ ) is given by :

$$z = (2Dt_p)^{\frac{1}{2}}. \quad (5)$$

z determines the temperature profile.

The condition  $\alpha^{-1} \ll z$  is applicable typically for laser irradiation of metals.

For laser irradiation, the beam intensity I at a depth z for the normally incident beam of initial intensity  $I_0$  (w/cm<sup>2</sup>) is given by:

$$I(z, t) = I_0(t)(1 - R)\exp(-\alpha z) \quad (6)$$

where R represents the reflectivity and  $\alpha$  is the absorption coefficient. Since  $\alpha$  is very high for metals,  $10^6 \text{ cm}^{-1}$ , light is totally absorbed within a depth of 100-200 Å.

The efficiency of optical coupling is determined by the reflectivity. R for metals is relatively low at short wavelengths, rises abruptly at a critical wavelength (related to the plasma frequency of the free electron plasma), and remains very high at long wavelengths.

When a laser beam heats the material, laser energy is first absorbed by free electrons. The absorbed energy then propagates through the electron subsystem and is transferred to the lattice.

Three characteristics time scales are:  $T_e$  – the electron cooling time, which is on the order of 1 ps;  $T_i$  – the lattice heating time; and  $T_l$  – the duration of laser pulse.  $T_e$  and  $T_i$  are proportional to their heat capacity divided by the same constant, and the heat capacity of electron is much less than that of lattice; therefore,  $T_e \ll T_i$ .

Laser beam interaction with the metals is basically a photo-thermal process governed by the heat equation:

$$\rho C_p \frac{\partial T}{\partial t} = K \nabla^2 T + P(x, y, z, t) \quad (7)$$

where  $\rho$  is the density of the material under consideration,  $C_p$  is the specific heat of the material,  $T$  represents temperature and is a function of position and time,  $K$  thermal conductivity of the material,  $P$  is the volume heat generation rate.

In laser machining using a Q-switched laser with pulse width on the order of nanoseconds, the primary material removal mechanism is ablation, but substantial melting is still present if a metallic material is concerned. The time for energy transfer from electron to lattice  $\tau_{lattice}$  is on the order of  $10^{-12}$  s. So, for the 50 ns pulse duration time, which is about 50 000 times of  $\tau_{lattice}$ , the electron gas temperature and the lattice temperature in the target material are about the same, and thermal equilibrium can be assumed. As a result, traditional heat transfer can be safely applied to laser machining using nanosecond pulses.

The models of Q-sw laser machining take into consideration effects of gas dynamics and Knudsen layer discontinuity during the ablation process. These models assume one-dimensional heat transfer in target material, recognizing that the machining depth is much smaller than the diameter of the hole, which is reasonable for relatively large holes (a few hundred microns). As a result, however, the effects of beam profiles and cavity profiles are not considered. These factors are important when the size of the hole is comparable to the drilling depth. The significant challenge in the thermal aspect at this time scale is how to model ablation and melting together. Also proper boundary conditions and property discontinuity at the liquid/vapor interface and laser/plasma interaction are necessary to be considered. The model in this paper concentrates on heat transfer and associated phase changes inside the target material. Stefan and kinetic boundary conditions are applied at the liquid-vapor interface, and property discontinuity across the Knudsen layer is considered.

Heat conduction is calculated using the enthalpy method. Most importantly, the axis symmetric model allows considerations of laser beam distribution and its coupling with the target material, which is important when the ablation extent is in the same order as the ablation depth.

Under the irradiation of a laser beam, target material is first heated from room temperature to melting temperature, at which point melting takes place. Depending on laser intensity and material properties, the molten part of material will be evaporated by additional heating when it reaches the vaporization point and a vapor-filled cavity is formed. A thin, so-called Knudsen layer exists at the melt-vapor interface, where the state variables undergo discontinuous changes across the layer. When the incident laser intensity exceeds a certain threshold, vaporization leads to plasma formation, which will absorb a certain percentage of laser energy. The more the intensity goes beyond the threshold, the denser the plasma, and the more percentage of absorption.

In practice, an assisting gas jet could disperse the plasma plume sideward and lower the plasma density, but the plasma effects still exist. By introducing a correction coefficient in the modelling of laser intensity, the plasma effects are corrected for.

The governing equation for energy balance can be written as:

$$\frac{\partial h'}{\partial t} + \frac{\partial \Delta H}{\partial t} = \frac{\partial}{\partial x'} \left( \alpha' \frac{\partial h'}{\partial x'} \right) + \frac{1}{r} \frac{\partial}{\partial r} \left( r \alpha' \frac{\partial h'}{\partial r} \right) \quad (8)$$

where  $\alpha'$  is heat diffusivity,  $\rho$  is density, and  $x'$  and  $r$  are distances along axial and radial directions.

The enthalpy of the material (the total heat content) can be expressed as  $H = h' + \Delta H$ , i.e., the sum of sensible heat,  $h' = cpT$  ( $cp$  is the heat capacity, and  $T$  is the temperature), and latent heat  $\Delta H$ . It either varies with  $Lm$ , the latent heat for melting, or is zero.

The enthalpy formulation allows one to trace the melting boundary as functions of time without regeneration of calculation grids.

The boundary conditions are given by :

$$Q + k \left( \frac{\partial T}{\partial x} + r \frac{\partial T}{\partial r} \right) + \rho_l v_l L_v - \rho_v v_v (c_p T_i + E_v) = 0 \quad (9)$$

$$E_v = \frac{RT_v}{(\gamma - 1)M_v} + \frac{1}{2} v_v^2 \quad (10)$$

$$Q = C(1 - R_l)I(t)e^{-\left(\frac{r}{b}\right)^2} e^{-\beta x} \quad (11)$$

where  $Q$  is the laser heat flux, which depends on reflectivity  $R_l$ , absorptivity  $\beta$  and the plasma correction coefficient  $C$ .  $I$  is the laser intensity which is a function of time, and  $b$  is the laser beam radius. The subscripts  $l$ ,  $v$  and  $i$  denote liquid phase, vapour phase, and vapour-liquid interface, respectively. The gas energy  $E_v$  includes the internal energy and the kinetic energy.  $k_c$  is the heat conductivity,  $v$  the velocity,  $R$  the universal gas constant,  $\gamma_h$  the specific heat ratio,  $L_v$  the latent heat of vaporization, and  $M_v$  the molecular mass. The velocity, the laser energy flux, and the heat conduction flux are valued along the normal direction of the cavity profile. The vapour-liquid front is determined by tracing the temperature. As long as the temperature at certain grid points reaches vaporization temperature, the grids which have temperatures larger than vaporization temperature are taken out as the gas phase and the calculation starts from the newly determined vapour-liquid front.

In the case when  $T_l \ll T_e \ll T_i$ , where  $T_l$  is of femtosecond scale, and laser pulse duration is shorter than the electron cooling time, electrons are heated instantly, then, in about 1 ps, electrons transfer their energy to their positive lattice ions. When this energy intensity is high enough, which is often true for ultrafast pulsed lasers, those ions get energy high enough to break the bonding of the lattice structure. They break off instantly without having time to transfer their energy to their neighbouring lattice ions; thus, direct solid-vapour transition occurs. Heat conduction into the target can be neglected; the heat affected zone is greatly reduced. For melting-free ablation to be possible, two conditions must be met: ultrashort pulse duration and high enough pulse energy. Since direct solid-vapour transition can be achieved so that all processes such as cutting, drilling, grooving, marking, or scribing can be used in this time region, and precise material removal is possible.

For ultrashort pulsed laser machining (10 ps or less), the material can be ablated precisely with little or no collateral damage. When a laser beam interacts with a material, electrons are excited by the absorption of photons. The electrons are heated to high temperature by absorbing laser energy through collisions with ions. Subsequent electron-photon interactions allow the absorbed energy to be transferred to the lattice in a time frame of picoseconds for most materials. For femtosecond pulses, there is insufficient time for energy transfer to the lattice; consequently, thermal damage is minimal.

Because the extreme intensity of the light, along with its short time frame compared with classical heat transfer, the thermal problems are quite different in ultrashort laser machining due to the two following effects.

### ***Thermal diffusion effect***

The difference in short- and long-pulse laser processing of materials begins with the way the laser pulse energy is deposited in the target material. Initially, the laser energy is deposited in the optical skin depth  $l_s = 1/\beta$ , where  $\beta$  is the absorption coefficient of the material. During the laser irradiation, the deposited energy is also transferred out of this layer to a depth given by the heat diffusion layer  $l_d = \sqrt{DT_l}$ , where  $D$  is the heat diffusion coefficient, and is  $T_l$  the laser pulse width. When the laser pulse width  $T_l$  is long so that  $l_d > l_s$ , laser processing is in the long-pulse regime. If the pulse width is so short such that  $l_d < l_s$ , the heat diffusion depth is limited to the very small skin depth. In metals, laser energy is absorbed by free electrons via the inverse Bremsstrahlung process in a skin layer of order of 10 nm. The electron-electron relaxation rate depends on the energy accumulated in the electron gas during laser heating. This is the regime of ultrashort-pulse laser processing. For ultrafast laser processing, the nonspread of the deposited laser energy causes rapid vaporization of the material.

Laser drilling and cutting with ultrashort laser pulses are therefore through direct evaporative ablation.

### ***Nonlinear absorption***

This is the second factor that contributes to production of smaller interaction volumes. Multiphoton absorption and avalanche ionization are insignificant at low intensities, but become increasingly probable at the gigawatt- and terawatt-per-square centimeter intensities, which these lasers create partially because of the ultra short pulse width involved.

Due to the very short time scales involved in the ablation with femtosecond laser pulses, the ablation process can be considered as a direct solid-vapour transition.

During all these processes, thermal conduction into the target can be neglected in a first approximation. This model works well for the metals and may be sufficient for materials with a significant band gap. However, this model assumes that reflectivity is constant and does not consider carefully the effect of nonlinear absorption on the ablation volume (multiphoton absorption and avalanche ionization).

It assumes that the thermalization within the electron subsystem is very fast, and that the electron and the lattice subsystems can be characterized by their temperatures ( $T_{electron}$  and  $T_{lattice}$ ). The energy transport into the metal can be described by the following one-dimensional, two temperature diffusion model:

$$Q(z) = -k_e \frac{\partial T_e}{\partial z} \quad (12)$$

$$S = I(t)A\beta \exp(-\beta z) \quad (13)$$

For femtosecond pulses, the laser pulse duration is much shorter than the electron cooling time,  $T_l \ll T_e$ . The electron-lattice coupling can be neglected. After the laser pulse, the electrons are rapidly cooled due to the energy transfer to the lattice and heat conduction into the bulk. The condition for strong evaporation is

$$F_a \geq F_{th} \exp(\beta z), \quad (14)$$

where  $F_{th} \cong \rho\Omega/\beta$  is the threshold laser fluency for evaporation with femtosecond pulses.

Then the ablation depth per pulse is:

$$L \cong \beta^{-1} \ln(F_a/F_{th}) \quad (15)$$

### **3. Experimental results**

Lasers help to enable economical volume manufacturing of various types of products.

### 3.1. Solar cells

These p-doped wafers are coated with an outer layer of n-doped silicon to form a large area p-n junction. But this thin (10-20 microns) layer coats the entire wafer, including the edges. To prevent front rear electrical leakage, a groove is continuously scribed completely through the n-type layer near the edge of the cell, in a process called Edge Isolation.

In order to maximize overall cell efficiency, this groove has to be as narrow and as close to the edge as possible. So manufacturers who first used 1064nm Qswitched DPSS lasers are increasingly turning to 532 nm and 355 nm lasers, because these lasers can scribe narrower grooves. In addition, 1064 nm laser ablation of silicon can create microcracks that emanate from the scribed groove. If these reach the edge of the wafer, structural integrity is potentially compromised. So this limits how close the 1064 nm-machined trenches can be placed to the edge of the wafer.

Gen II devices based on thin-film technology are often ‘rear-side’ devices in which sunlight enters through a glass ‘superstrate’ that acts as the support for layers of transparent conductive oxide (TCO), the active semiconductor layer (a-silicon, CdTe or CIG S) and then a metal layer (typically aluminium electrodes). After each layer is deposited, it must be scribed in order to divide the large area panels into discrete, isolated solar cells and to define the interconnects which link the cells together. This is actually done through the glass superstrate. The TCO is scribed (the P1 process) using a 1064 nm laser.

The other scribes (P2 and P3) are performed using a 532 nm laser which passes through the TCO and is strongly absorbed at the TCO-semiconductor interface, causing a “micro-explosive” effect that cleanly lifts the semiconductor layer – plus the overlying metal layer in the case of P3. As with Gen I, it’s vital to minimize space wasted by the scribes. This requires narrow scribes with a minimized HAZ (heat affected zone). These two applications are best supported with lasers that combine high (100 kHz) pulse repetition rate necessary for economic scribing with a short pulse duration that results in a minimized HAZ.

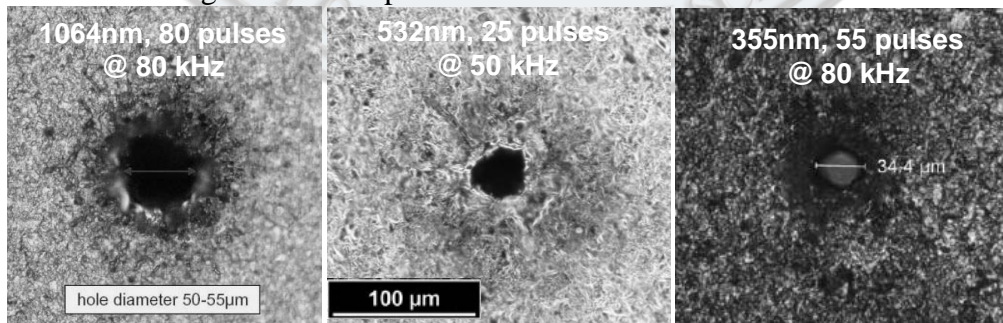


Fig. 1. Different steps in manufacturing solar cells

### 3.2. Laser Direct Patterning of Flex Circuits

Laser direct patterning (LDP) is now being used to produce dense PCB and flex circuits at low cost, for applications such as RFID and disposable medical sensors. It is already delivering 15 micron resolution, and is easily capable of going higher. It is compatible with several types of metals patterned on many common polymer substrates including Kapton®, Upilex®, Kaladex®, Melinex® and Mylar®. The first step is vapour deposition of a thin (<150 nanometer) layer of metal on to the polymer substrate. Next, a 308 nm excimer laser beam projects the image of a photomask onto this prepared metal surface. Because the metal layer is very thin, and metals generally don't have strong absorption in the UV, most of the ultraviolet laser light passes through it. But, organic polymers exhibit extremely strong UV absorption, so all the remaining laser light is completely absorbed in the uppermost layer of the polymer causing instantaneous ablation of the surface layer. This vaporization also removes the overlying metal film, leaving a metal pattern that corresponds to the photomask in every detail.

In order to support low-unit cost using fast reel-to-reel or roll-to-roll processing, the key laser requirement is very high pulse energy such as  $1\text{J}/\text{cm}^2$ . This allows an entire circuit or group of circuits to be patterned with a single laser pulse. This extremely high pulse energy means that for many polymers, an area of several hundred square millimeter can be patterned with a single laser pulse. And the short (< 25 ns) pulsewidth of this laser makes it compatible with continuous, high-speed reel to reel motion. Even with a modest repetition rate (e.g. 50 Hz), over 100,000 circuits/hour can be created with perfect pattern repeatability. Moreover, this huge volume of parts can be produced without any trade-offs in resolution, precision and feature definition.

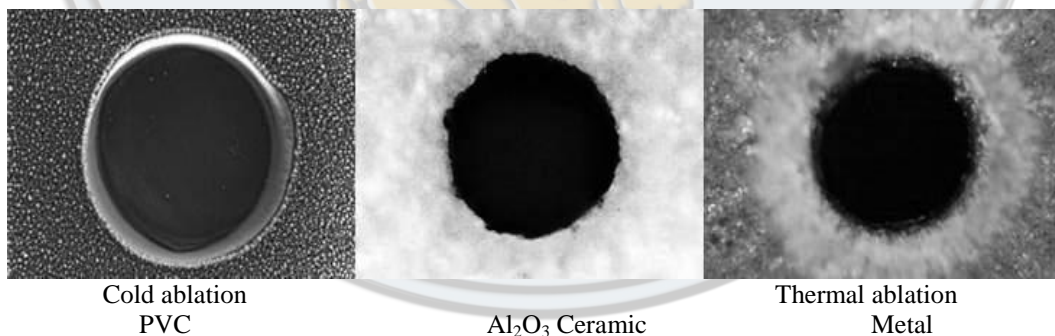


Fig. 2. Results that have been obtained using different materials

### 3.3. Engraving with CO<sub>2</sub> Lasers

In laser engraving, surface marks are produced by controlled material removal. Laser engraving applications include product/label personalization, product identification and brand labelling, manufacturing architectural signs, marking

trophies and plaques, and even creating photo-realistic headstones. Laser engraving represents a superior alternative to traditional mechanical engraving using a rotary tool. Specific advantages include consistent results with no tool wear, no tool replacement downtime, higher spatial resolution, digital control and flexibility and the ability to produce complex, even three-dimensional graphics. For example, many laser engraving machines now offer resolution of several hundred dpi, whereas even the best mechanical engraving machines are realistically limited to a few hundredths of an inch (10–50 dpi) at best.

Engraving applications typically employ a sealed-off CO<sub>2</sub> laser in the 10-100 watt power range. This offers the ideal combination of low cost per watt and superior beam quality. The infrared (10.6 micron) radiation is strongly absorbed by plastics, paper, glass and wood; even metals can be readily engraved by using a low cost surface coating to absorb at this wavelength. Laser systems should provide the high reliability these applications need; engraving tool builders often have hundreds of end users all over the world, each having just a single machine, so lasers requiring frequent service would be economically and practically unacceptable.

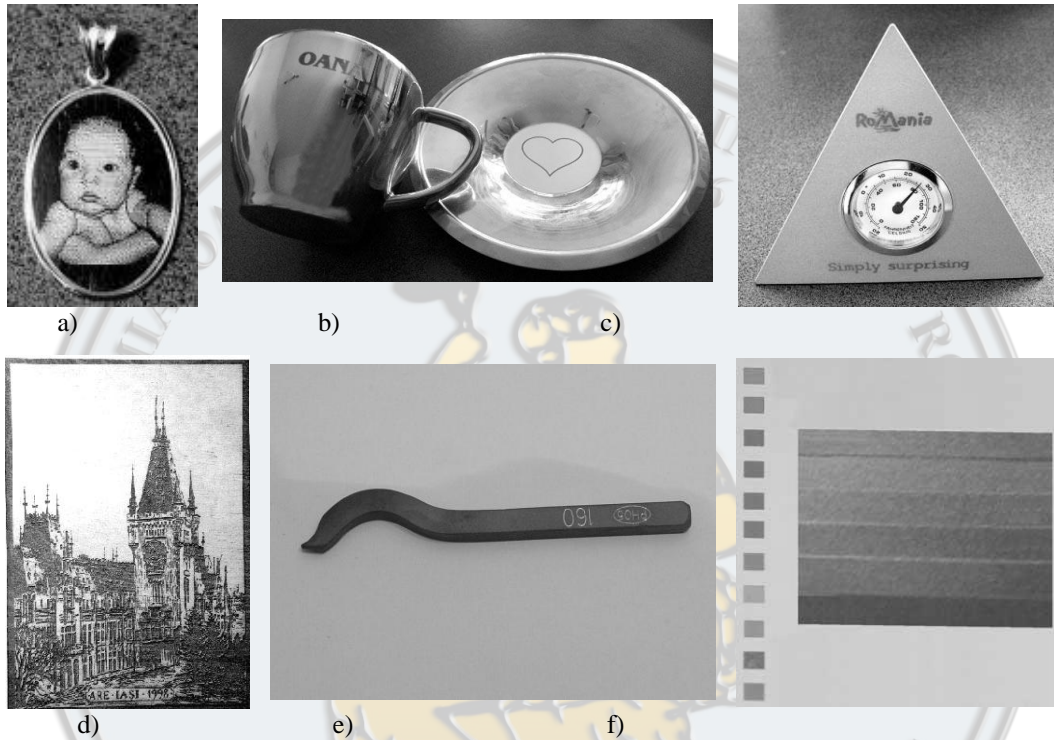


Fig. 3. Samples of promoting materials realized with a 60W CO<sub>2</sub> laser

### 3.4. Fiber Laser

Surface treatments of stainless steel in air were performed by scanning with a Yb ( $\lambda=1.064 \mu\text{m}$ ) pulsed laser beam at high repetition rate. Different coloured samples were obtained depending on the laser accumulated fluency. Although changes in the colours of the samples may be correlated with the coating composition, the influence of light interference within the thin surface layer should not be ignored. A thin oxide layer on the surface developed by controlled laser irradiation may produce a particular colour or luster. We suggest that colouring is due to photochemical activation, while photothermal oxidation is responsible for the bleaching process. In stainless steel, a thermochemical reaction between oxygen and stainless steel is believed responsible for colouring during laser irradiation in air. With increasing laser fluencies, the temperature rise in the irradiated area of stainless steel surface increases, which enhances oxygen

diffusion into the surface and oxidation reaction within the irradiated area. Thus, laser irradiation in vacuum is an easy way to avoid discoloration of stainless steel. In order to identify the electronic process involved in colouring, we have carried out single-colour femtosecond pump-probe experiments to investigate the time dependence of laser-induced ultrafast absorption and deformation processes. We have observed that at high frequencies the colour effect was minimal.



**Fig. 4.** Results

- a) the portrait of a baby on a gold jewellery
- b) an inox tea set
- c) clock
- d) a photo engraved picture on a brass plate
- e) a 3D engraving piercer for marking jewels
- f) colour spectrum

We have used a 10 W diode pumped Yb fiber laser, the highest frequency being 80 kHz. The used soft is SAMLight provided by SCAPS Company.

Properly applied laser coloration markings cannot be felt on a smooth surface when rubbed with the finger and appear smooth when viewed under low (10X) magnification. The laser colouring process is not recommended for parts thinner than 0.10", it uses slow speed and relatively low power.

Laser etching is similar to laser colouring except that the heat applied to the surface is increased to a level that causes substrate surface melting.

The advantage to using this technique over laser colouring is increased marking speed since the process needs less depth than is required to colour metallic substrates.

Excellent results can be routinely obtained at penetration depths of less than 0.001-inch.

Laser etched marking can generally be felt when rubbed with a finger and may have a corn row appearance when viewed under low (10X) magnification.

Laser etching is not recommended for parts thinner than 0.050”.

By contrast, on raw metal surfaces, a broad range of chromatic colours can be obtained, enabling use of Nd:YAG and Nd:YVO<sub>4</sub> lasers as a true decorative tool (see Figure 2 ).

In this case, the generation of different colours is linked to the surface diffraction grid obtained by means of several laser passages performed on the same area but with different laser parameters.

A laser to be used for this type of work must be able to be tuned to operate at a broad range of frequencies, speeds, power levels, fill spacing settings, focal distances, and so on.

### 3.5. 3D Glass Laser Processing

In the case of glass laser processing we have to take into consideration also the shockwave mechanism.

The Toshiba Company has for the first time obtained a shock laser treatment using a 532 nm electromagnetic wave and a focal size spot of 700  $\mu$  m.

It was observed that the laser energy was converted more into a mechanical wave than into a thermal process.

From this point it was started the study of interaction between laser and transparent materials.

Usually the whole energy is absorbed into a tiny layer that is quickly vaporized and ionized and by this mechanism a plasma plume is formed. At its turn it gives born to a pressure wave [7].

The major physical process is the inverse bremsstrahlung.

The pressure wave is proportional with square root of intensity up to a point where it reaches the saturation. Also we have to bear in mind that it is necessary a time period so that the effect should be permanent and at this point it interferes also the elasticity constant of the material. So the pulse duration is best to be between 3 - 10 ns.

The saturation of the pressure depends also by the wavelength; the shorter the latter the intensity value at which the breakdown appears is smaller:  $2 \text{ GW/cm}^2$  at 308 nm,  $4 \text{ GW/cm}^2$  at 355 nm,  $6 \text{ GW/cm}^2$  at 532 nm and  $10 \text{ GW/cm}^2$  at 1064 nm.

At a first glimpse the 532 wavelength has the biggest advantage because it reaches equilibrium between all the parameters.

Depending of the wavelength there are different physical processes. In the IR case the electronic avalanche is dominant while for UV/VIS region we are dealing with a multiphotonic ionization.

A laser engraving machine may be considered of as three main parts: a laser as shown in Figure 6, a controller (usually a computer), and a surface.

Direction, intensity, speed of movement, and spread of the laser beam aimed at the surface are usually controlled by the computer.

Of course there are some requirements for marking objects using this technique: the surface of the object must be plain and polished; also the absorption must be less than  $0.01 \text{ cm}^{-1}$  at 532 nm.

An optical crystal has a  $4.5 \text{ g/cm}^3$  and a melting temperature of  $1970 \text{ C}^0$  towards the usual values for the BK7 glass eg.  $2.5 \text{ g/cm}^3$  and  $1200 \text{ C}^0$ . The results are shown in Fig. 5.

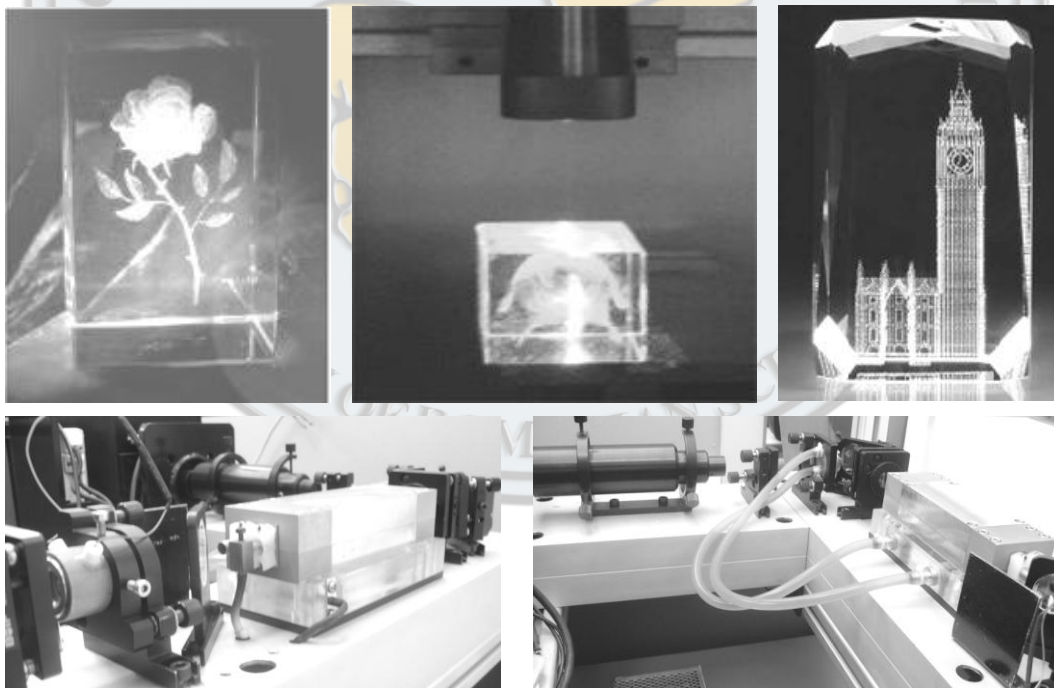


**Fig. 5.** 3D Glass Engraving and the Nd:YAG Laser

## REFERENCES

- [1] Valerică Ninulescu, Andreea Rodica Sterian, *Dynamics of a Two – Level Medium Under the Action of Short Optical Pulses*, Computational Science and Its Applications – ICCSA – 2005, Gervasi et al. (Eds): Lecture Notes in Computer Science (ISI web off Science), LNCS 3482, pp. 635- 642, Springer – Verlag, Berlin, Heidelberg, 2005.
- [2] Valerică Ninulescu, Andreea Rodica Sterian, *Nonlinear Phenomena in Erbium – Doped Lasers*, Computational Science and Its Applications – ICCSA – 2005, Gervasi et al. (Eds): Lecture Notes in Computer Science (ISI web off Science), LNCS 3482, pp. 635- 642, Springer – Verlag, Berlin, Heidelberg, 2005
- [3] F.C. Maciuc, C.I. Stere, Andreea Rodica Sterian *Time evolution and multiple parameters variations in a time dependent numerical model applied for  $Er^{+3}$  laser system*, Proceedings of Spie (ISI Proceedings), “Laser Physics and Applications”, Vol. 4394, 2001, pp.84-89
- [4] Dan.C. Dumitras, *Ingineria fasciculelor laser*, Editura All, 2004
- [5] Stuart et. al., Phys.Rev. Lett., 74, 2248(1995)
- [6] Lenzer et. al, Phys, Rev. Lett., 80, 4076 (1998)
- [7] Glezer et. al., Appl. Phys. Lett., 71, 882 (1997)
- [8] <http://www.mrl.columbia.edu/Time%20scale%20effects.pdf>
- [9] [http://www.orc.soton.ac.uk/publications/theses/2729\\_jaac/CHAPTER8.pdf](http://www.orc.soton.ac.uk/publications/theses/2729_jaac/CHAPTER8.pdf)
- [10] <http://www.ias.ac.in/sadhana/Pdf2003JunAug/Pe1103.pdf>
- [11] <http://arxiv.org/ftp/arxiv/papers/0704/0704.0701.pdf>